Angular Gaps in Radial Diffusion-Limited Aggregation: Two Fractal Dimensions and Nontransient Deviations from Linear Self-Similarity

Benoit B. Mandelbrot,[1] Boaz Kol,[2] and Amnon Aharony[2]

[1]*Department of Mathematics, Yale University, New Haven, Connecticut 06520-8283*

[2]*School of Physics and Astronomy, Raymond and Beverly Sackler Faculty of Exact Sciences, Tel Aviv University, Tel Aviv 69978, Israel*

(Received 23 September 2001; published 15 January 2002)

When suitably rescaled, the distribution of the angular gaps between branches of off-lattice radial diffusion-limited aggregation is shown to approach a size-independent limit. The power-law expected from an asymptotic fractal dimension $D = 1.71$ arises only for very small angular gaps, which occur only for clusters significantly larger than $M = 10^6$ particles. Intermediate size gaps exhibit an effective dimension around 1.67, even for $M \to \infty$. They dominate the distribution for clusters with $M < 10^6$. The largest gap approaches a finite limit extremely slowly, with a correction of order $M^{-0.17}$.

DOI: 10.1103/PhysRevLett.88.055501 PACS numbers: 61.43.Hv, 05.45.Df, 47.53.+n

For years, a considerable effort has been devoted to the numerical analysis of diffusion-limited aggregation (DLA) [1], a model of many natural fractal growth processes. Even though DLA has no characteristic length scale, simulations exhibit nontrivial and ambiguous characteristics [2,3]. In the plane, the fractal dimension $D = 1.71$ is usually associated with radial DLA [4], and $D = 1.66$ is associated with cylindrical DLA [5–8].

Although the mass of radial DLA obeys the relation $M \sim R_g^{1.71}$ (R_g is the radius of gyration) for all R_g's, its geometry varies with R_g [9]. Figure 1 compares two DLA clusters: One recognizes about $\mathcal{N} = 5$ main arms for $M = 10^5$ particles [10], but $\mathcal{N} = 8$ or 9 for $M = 10^8$ [9]. This makes the $M = 10^8$ cluster look more dense (like a filled circular disc) [2,3]. However, different interpretations of $\mathcal{N}$ lead to contradictory results. Lacking meaningful ways to analyze data, there have been very few publications on numerical analysis of DLA since 1995. Here we present a new systematic description that incorporates the arms in a broad context: we study the statistics of *all the angular gaps between branches*. While Ref. [9] pioneered such gap analysis, it had insufficient data and no data collapse. Application of the "ϵ-neighborhood" analysis related the increase in $\mathcal{N}$ (and in the apparent density) to an increasing *lacunarity,* which could remain consistent with $M \sim R_g^{1.71}$. The two scenarios proposed there — long transient and infinite drift — should be replaced by a subtle new one, described here.

Our principal new finding is that, under appropriate scaling, and apart from finite size tails, the distributions of gap sizes for different M's collapse onto a single function, which should also characterize most of the gaps in the limit $M \to \infty$. Intermediate size gaps exhibit an effective dimension around 1.67, and one needs very small gaps, hence very large clusters, to observe the widely anticipated asymptotic behavior with the unique dimension $D = 1.71$. Interestingly, the two widely quoted values of D are *both* present in radial DLA.

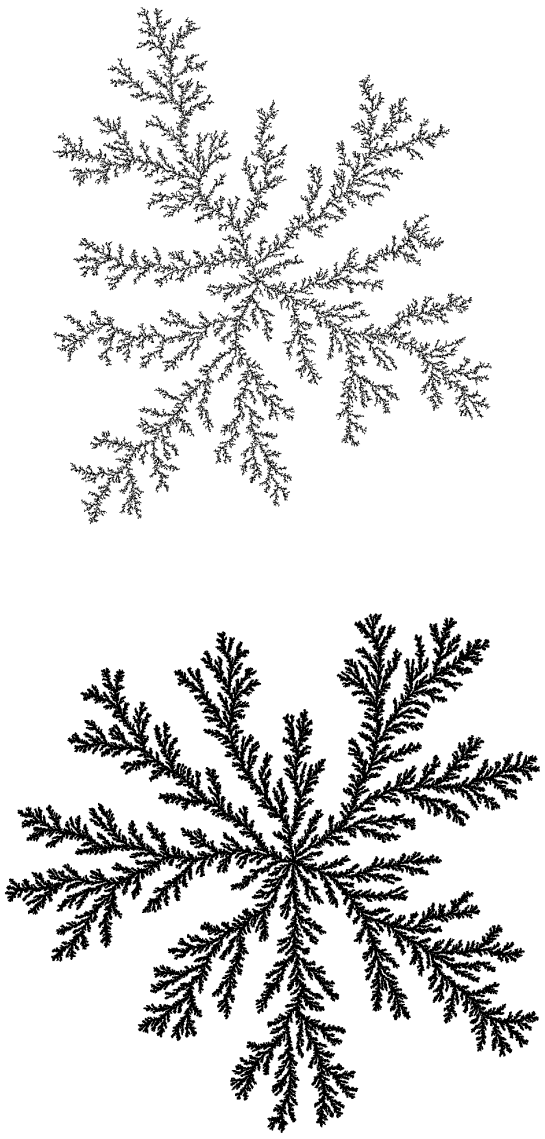

FIG. 1. Two radial DLA clusters, with $M = 10^5$ (top) and $M = 10^8$ (bottom) particles.

The intermediate dimension $D \sim 1.67$ is *not* a small sample correction to asymptotic self-similarity. Indeed, the number of gaps in this zone changes little with M, and they remain observable for *all* M. Therefore, DLA cannot be modeled by a unique fractal dimension, that would correspond to a fractal that is invariant under *linear* transformations. For many phenomena, such as percolation, random forms of such "linear fractals" are good models and nonrandom linear fractals provide illuminating "cartoons." In contrast, DLA (and probably other phenomena) require steps beyond linear self-similarity. Our procedure suggests such a quantitative step.

The data collapse of the gap distribution implies that typically, the largest angular gap (which gives some measure of $\mathcal{N}$) approaches a *finite* limit, which seems to be nonzero. However, there is an amazingly slow correction, of order $M^{-\gamma}$, where $\gamma = (2 - D)/D = 0.17$. This correction may or may not be related to the corrections recently found using a conformal map approach [11,12].

We performed large scale simulations of off-lattice radial DLA, and focused on the gaps on circular cross-cuts. An earlier analysis [3], based on $M \leq 10^7$, yielded an apparent fractal dimension $D = 1.65 \pm 0.01$, which is not consistent with the widely accepted $D = 1.71$. Our software is as described in Ref. [13], but uses a single diffusing particle each time, as in the definition of DLA [1]. We generated $N_c(M) = 1000$ clusters for each of the "masses" $M = 10^5, 10^{5.5}, 10^6, 10^{6.5}$, and 10^7, plus $N_c(M) = 60$ additional clusters for $M = 10^{7.5}$ and for 10^8.

After growing several DLA clusters, we endeavored to keep to the edge of the nongrowing region. Trial and error [2,3] singled out particles whose distance R from the origin is within $0.75R_g - 1 < R < 0.75R_g + 1$ (in units of the particle diameter). The gap θ is the difference in the polar angles between consecutive particle centers. To avoid "gaps" between touching particles, we keep only the values $\theta > 1/0.75R_g$, larger than one particle diameter. We then pool the gaps from all the available clusters of size M into a single list, which is sorted from largest to smallest. Thus each gap is characterized by its size and by an integer r that represents its rank in the sorted list. Here we use the mean rank, $\rho \equiv r/N_c(M)$, which becomes an M-independent continuous variable for $N_c \to \infty$.

For an ideal linearly self-similar fractal of dimension D, one expects a power law $\theta \propto \rho^{-\alpha}$, where $\alpha \equiv 1/D_c$ and $D_c \equiv D - 1$ is the fractal dimension of the intersection [14]. In contrast, Fig. 2 shows that $\theta(\rho, M = 10^8)$, based on the available $N_c(10^8) = 60$ clusters, exhibits four distinct regions: region I, with $\rho < 10$, reflects the statistics of the largest gaps. As in the Zipf-Mandelbrot distribution [14], the flattening of the curve in this region is a token of an upper cutoff (though not necessarily a sharp one) on the size of gaps. Both regions II and III appear to be linear (see dashed lines in Fig. 2). In region II, with $10 < \rho < 50$, the apparent slope is $\alpha_{\rm II} \cong 1.5$, corresponding to $D_{\rm II} \cong 1.67$. In region III, with $50 < \rho < \rho_{\max}/3$, where

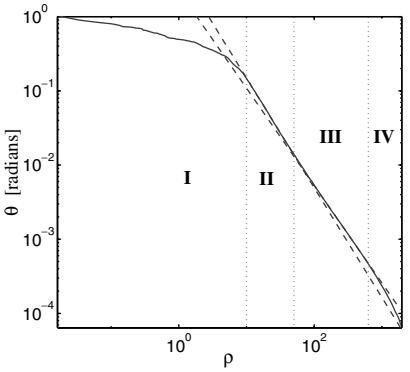

FIG. 2. The gap size θ vs the mean rank ρ. The graph is based on 60 clusters with 10^8 particles. The dotted vertical lines separate the four regions discussed in the text. Dashed straight lines run through regions II and III.

$\rho_{\max}(M = 10^8) = 1890$ is the maximal ρ for which θ is defined (i.e., the average total number of gaps), the apparent slope is $\alpha_{\rm III} \cong 1.33$, corresponding to $D_{\rm III} \cong 1.75$. Region IV, with $\rho_{\max}/3 < \rho < \rho_{\max}$, reflects finite-size corrections: as $M \to \infty$ one has $\rho_{\max} \to \infty$, and (as far as we can tell) region III extends to infinity, reflecting the asymptotic behavior of DLA. Since $\rho_{\max}$ increases with M, it also follows that for M smaller than about 10^6, region III merges with region IV, and one would mistakenly identify D from the higher apparent slope of region II. This clearly demonstrates why one must have very large clusters to make statements about the asymptotic behavior of DLA.

Visually, region I defines the arms. As $M \to \infty$, region III collapses into the observed thickening "trunks." Region II determines the structure of the clearly separate intermediate branches, which exist for all M.

A quantitative way to describe the crossover between regions II and III would involve corrections to the asymptotic power law. Lacking enough data, we represent the data we have by an *ad hoc* parametric power expansion $\theta(\rho) = \sum_{k=1}^{k_{\max}} a_k \rho^{-k\alpha} = \sum_{k=1}^{k_{\max}} a_k x^k$, where $x = \rho^{-\alpha}$. Using $\alpha = 1.4$, this form ensures the asymptotic dimension $D = 1.71$ for large ρ. A least squares fit with $k_{\max} = 6$ to the data for $10 < \rho < \rho_{\max}/3$ at $M = 10^8$ yields $a_k = 3.702, -126.7, 1.566 \times 10^4, -8.045 \times 10^5$, 1.901×10^7, and -1.694×10^8. The approximate effective dimension, $D_{\rm eff}(\rho) \equiv 1 + 1/\alpha_{\rm eff}$, where $\alpha_{\rm eff}(\rho) \equiv -d(\log\theta)/d(\log\rho) = \alpha \frac{x}{\theta} \frac{d\theta}{dx}$, is shown in Fig. 3. Indeed, $D_{\rm eff}$ reaches a minimum of about 1.66 close to $\rho = 20$ (in region II), and a maximum of about 1.74 around $\rho = 80$ (in the beginning of region III). It approaches the asymptotic $D = 1.71$ at larger ρ.

To demonstrate scaling and data collapse, we scale θ as

$$\theta(\rho, M) = S(M)\theta_n(\rho), \tag{1}$$

$$S(M) \equiv \int_0^G \theta(\rho, M)\, d\rho\,. \tag{2}$$

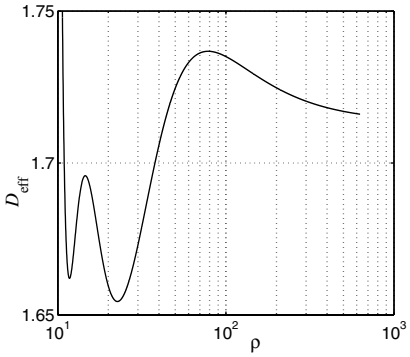

FIG. 3. Effective dimension $D_{\rm eff}(\rho)$.

$S(M)$ represents the largest gaps. G should be large enough in order to filter more of the statistical variance, but not too large as to include finite-size corrections. The results are not very sensitive to G (see below). The choice $G = 50$, at the beginning of the asymptotic slope (region III), gives good results and facilitates some of the theoretical analysis presented later. Figure 4 shows that $\theta_n(\rho, M)$ is indeed independent of M, except for finite-size correction deviations.

The curves in Fig. 4 end at $\rho_{\rm max}(M)$. The figure clearly shows fixed distances between consecutive end points, indicating power-law dependence of both $\rho_{\rm max}$ and of $\theta(\rho_{\rm max})$ on M. Since $\rho_{\rm max}$ is the average number of gaps (or particles) on the annulus of radius R, we expect $\rho_{\rm max} \propto R^{D-1} \propto M^{(D-1)/D}$. The smallest gap is then expected to scale as $1/R \propto 1/M^{1/D}$. We thus expect the small gaps to scale as

$$\theta(\rho, M) = M^{-1/D} f(\rho^{1/(D-1)}/M^{1/D}). \qquad (3)$$

Indeed, Fig. 5 shows $M^{1/D}\theta$ plotted vs $\rho^{1/(D-1)}/M^{1/D}$ for various M's. There is a clear data collapse on the right-hand side, in agreement with Eq. (3).

We next use the collapse of the normalized gaps in Fig. 4 to infer the asymptotic distribution of the original (non-normalized) gaps as a function of M. As expected for $\rho < \rho_{\rm max}/3$, θ_n depends only on ρ, and *not* on M. The M dependence of the original gaps, $\theta(\rho, M) = S(M)\theta_n(\rho)$, is thus determined by the scale factor $S(M)$. Integrating over ρ on both sides of Eq. (1), the left-hand side becomes $\int_0^{\rho_{\rm max}} \theta(\rho, M) = 2\pi - X$, equal to the average sum (over all cluster realizations) of all the gaps; X is the sum over the gaps that are smaller than one particle in diameter. We expect $X \propto \rho_{\rm max}/R_g$, and therefore $X = B_1 M^{-\gamma}$, with $\gamma \equiv (2 - D)/D = 0.17$. On the right-hand side, we divide the integral into three parts: $0 < \rho < G$, $G < \rho < \rho_{\rm max}/3$, and $\rho_{\rm max}/3 < \rho < \rho_{\rm max}$. Equation (2) implies that $\int_0^G \theta_n \, d\rho \equiv 1$. The second integral belongs to region III, where we write $\theta_n(\rho) \simeq A_1 \rho^{-\alpha}$, and $A_1 = a_1/S(10^8) = 0.77 \pm 0.01$ is independent of M (as seen from Fig. 4). This yields $B_2[G^{-\beta} - (\rho_{\rm max}/3)^{-\beta}]$, with $\beta = (2 - D)/(D - 1)$ and $B_2 = A_1/\beta$. Since $\rho_{\rm max} \propto M^{(D-1)/D}$, we conclude that the integral over the right-hand side is equal to $S(M)\,(A - B_3 M^{-\gamma})$, where $A = 1 + B_2 G^{-\beta} = 1.40 \pm 0.01$ and B_3 is a constant [which is also affected by $\int_{\rho_{\rm max}/3}^{\rho_{\rm max}} \theta_n \, d\rho \sim M^{-\gamma}$, due to Eq. (3)]. Our conclusion is that for large M one has

$$S(M) = \frac{2\pi - B_1 M^{-\gamma}}{A - B_3 M^{-\gamma}}, \qquad (4)$$

and hence $\theta(\rho, M = \infty) = (2\pi/A)\theta_n(\rho) \cong 4.5\theta_n(\rho)$.

While the distribution of gaps does converge to a limit for $M \to \infty$, this convergence is *amazingly* slow, being governed by the small exponent γ: The correction term in Eq. (4) reduces only by a factor of $10^{3\times 0.17} \simeq 3.2$, between $M = 10^5$ and $M = 10^8$. This means that great caution should be taken when extrapolating various measurements in DLA, and that the asymptotic limit is attained only for extremely large M.

We next examine the statistics of the largest gaps, $\theta_{\rm max}$. For a linearly self-similar fractal, one expects to find the same distribution of the $\theta_{\rm max}$'s for different cluster sizes. $\theta_{\rm max} \approx 2\pi/\mathcal{N}$ may indicate that the number of main branches is around $\mathcal{N}$. It has been shown that $\theta_{\rm max}$ decays slowly with M [3], which means that $\mathcal{N}$ increases,

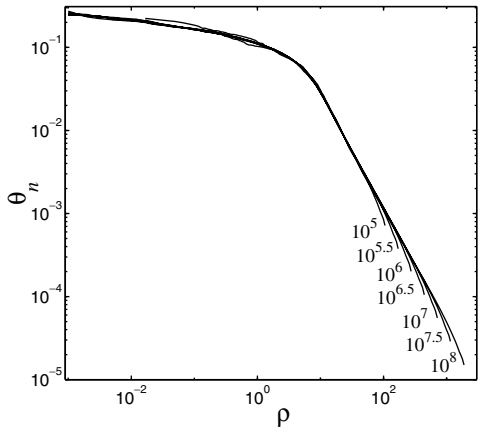

FIG. 4. Data collapse of $\theta_n(\rho, M)$. The numbers indicate the cluster size M.

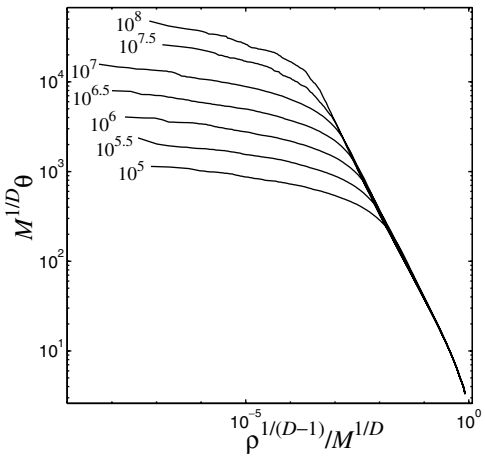

FIG. 5. $M^{1/D}\theta$ vs $\rho^{1/(D-1)}/M^{1/D}$ for various values of M.

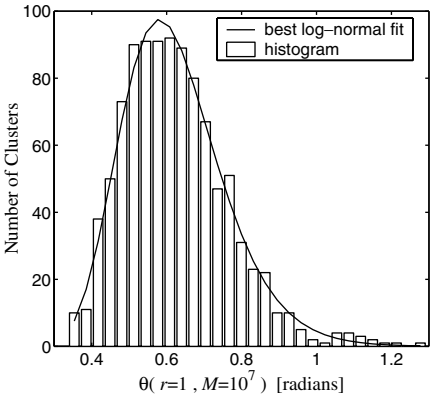

FIG. 6. Histogram of the maximal gap (in radians) in each cluster, for the 1000 available clusters with $M = 10^7$.

raising doubts on the self-similarity of DLA at intermediate values of M.

If, instead of pooling, we had studied the gaps of a single cluster, then we would have $\theta_{\max} = \theta(r = 1)$. However, the mean-rank $\rho = 1$ has a different meaning: $\theta(\rho = 1, M)$ is the N_cth largest gap out of all the gaps taken from N_c clusters. Since the graph of $\theta_n(\rho, M)$ is relatively flat near $\rho = 1$, we still expect $\theta(\rho = 1, M)$ to represent the order of magnitude of the average largest gap. Reading $\theta_n(\rho = 1) = 0.1$ from the universal curve in Fig. 4, we estimate $\theta(\rho = 1, M = \infty) = (2\pi/A)\theta_n(1) \cong 0.45$, in radians, yielding an asymptotic average maximal gap around 26° and implying a finite number of arms.

The histogram of the $\theta_{\max}$'s for different clusters with $M = 10^7$ is shown in Fig. 6. It is quite broad. A fit to a log-normal form (also shown) yields $\mu = \langle \ln\theta_{\max} \rangle \cong -0.50$ and $\sigma = \langle (\ln\theta_{\max} - \mu)^2 \rangle \cong 0.22$. We find a very slow decrease of μ with M, approaching a finite limiting value of the order of magnitude given above.

The broad distribution of $\theta_{\max}$ implies that under pooling, the largest pooled gaps spread over a broad range of ρ. Pooling convolutes the distributions of two nonindependent quantities: the gaps for each cluster and the different clusters. For additional insight into these distributions, we also considered the correlations between gaps within each cluster. We find several interesting results: the average correlation between the largest gap and the rth gap for $M = 10^7$ turns out to decrease from 1 to 0 (around $r = 5$), and to approach a constant around -0.5 for $r > 10$. Negative correlations were expected, since the total sum of the gaps must equal 2π.

In collaboration of Eugene Vilensky of Yale, we also tested our results' sensitivity to the special choice of $R \sim 0.75R_g$. An increase of R beyond this value first leads to little change (confirming [2,3]), then to opposite changes in different regions: Very large gaps come to dominate in region I, moving the corresponding "flat" portion of the curve to higher values of θ. The remaining gaps (other than the few largest) add to a decreasing total angle, but with little change in distribution.

In conclusion, we have identified robust structural features of radial DLA, which act separately in characterizing the arms, the intermediate and the fine branches. Although all fall within a single scaling function, the nontrivial gap distribution function reflects deviations from simple linear fractality. Since these deviations characterize the radial geometry, it would be interesting to check if they also appear in the (possibly simpler) cylindrical case. This is particularly intriguing, since both involve $D \approx 1.66$. Finally, since our data "only" extend up to $M = 10^8$, there is no guarantee that this is the end of the story [15]. Future work should tell if larger scales bring more surprise.

Henry Kaufman kindly adapted his DLA program to serve our needs. This work has been supported in part by the German-Israeli Foundation (GIF).

[1] T. A. Witten and L. M. Sander, Phys. Rev. Lett. **47**, 1400 (1981); Phys. Rev. B **27**, 5686 (1983).
[2] B. B. Mandelbrot, H. Kaufman, A. Vespignani, I. Yekutieli, and C. H. Lam, Euro. Phys. Lett. **29**, 599 (1995).
[3] B. B. Mandelbrot, A. Vespignani, and H. Kaufman, Euro. Phys. Lett. **32**, 199 (1995).
[4] S. Tolman and P. Meakin, Phys. Rev. A **40**, 428 (1989).
[5] A. Erzan, L. Pietronero, and A. Vespignani, Rev. Mod. Phys. **67**, 545 (1995).
[6] P. Meakin and F. Family, Phys. Rev. A **34**, 2558 (1986).
[7] B. Kol and A. Aharony, Phys. Rev. E **62**, 2531 (2000).
[8] B. Kol and A. Aharony, Phys. Rev. E **63**, 046117 (2001).
[9] B. B. Mandelbrot, Physica (Amsterdam) **191A**, 95 (1992).
[10] A. Arneodo, F. Argoul, E. Bacry, J. F. Muzy, and M. Tabard, Phys. Rev. Lett. **68**, 3456 (1992).
[11] E. Somfai, L. M. Sander, and R. C. Ball, Phys. Rev. Lett. **83**, 5523 (1999).
[12] B. Davidovitch and I. Procaccia, Phys. Rev. Lett. **85**, 3608 (2000).
[13] H. Kaufman, A. Vespignani, B. B. Mandelbrot, and L. Woog, Phys. Rev. E **52**, 5602 (1995).
[14] B. B. Mandelbrot, *The Fractal Geometry of Nature* (Freeman, New York, 1982).
[15] Eden clusters reach asymptotia only for $M > 10^8$ [J. G. Zabolitzky and D. Stauffer, Phys. Rev. **34**, 1523 (1986)].